

# Development of a Pulsed Slowing-Down-Time Benchmark of Neutron Thermalization in Graphite

E. Lee, N. C. Fleming, A. I. Hawari

Department of Nuclear Engineering, North Carolina State University, Raleigh, NC 27695, USA  
[ele23@ncsu.edu](mailto:ele23@ncsu.edu), [ncsorrel@ncsu.edu](mailto:ncsorrel@ncsu.edu), [ayman.hawari@ncsu.edu](mailto:ayman.hawari@ncsu.edu)

## INTRODUCTION

Graphite is a classic neutronic material that has been used as both a reactor reflector and moderator in various nuclear reactor systems. The ability to accurately predict the slowing down and thermalization of neutrons in graphite can have significant implications on the safety and operation of such reactor systems. In reactors, the neutron thermalization process is quantified using the thermal scattering law (TSL) and related cross sections for a given moderator. An ideal approach to assess the validity of TSL data is using benchmark measurement based on the pulsed Slowing-Down-Time technique and its comparison with the appropriate graphite nuclear library [1,2].

In this work, experimental measurement and computational Monte Carlo simulations were performed to benchmark the slowing down characteristics and thermalization of neutrons in nuclear (reactor-grade) graphite. Given the density of graphite, various graphite libraries were selected for the benchmark analysis.

## Background on Slowing-Down-Time

The Slowing-Down-Time (SDT) technique focuses on the time spent by neutrons during their slowing down and thermalization process [1,2]. This technique is an integral benchmark technique based on the fundamental coupling between the energy of a neutron as it slows down in graphite and the time that is required to reach that energy. This unique coupling between the neutron energy and slowing-down-time allows identification of the moment in time when neutron reach a particular energy region, e.g., the thermal region. Once the neutrons reach thermal energies, their interaction is described by the thermal neutron scattering law (TSL, i.e.,  $S(\alpha, \beta)$ ) that contains the structural and dynamical information of a moderator, e.g., graphite [3].

The neutron slowing down process can be described as a continuous decrease in a relatively sharply defined neutron energy. Using computational simulations, the average energy of the neutrons during the slowing down process is given by

$$\bar{E}(t) = \int_E E \cdot \psi(E, t) dE, \quad (1)$$

$\psi(E, t)$  is the time-energy dependent neutron energy spectrum normalized to unity. Using equation (1), the time-

energy correlation can be established computationally to support interpretation of the benchmark data.

## NEUTRON THERMALIZATION IN GRAPHITE USING A SLOWING-DOWN-TIME EXPERIMENT

The SDT experiment was conducted at the Oak Ridge Electron Linear Accelerator (ORELA) facility, a part of Physics Division of Oak Ridge National Laboratory (ORNL). The experiment utilized the Slowing-Down-Time spectrometry to observe the behavior of ORELA neutron pulses that were running with a pulse frequency of 130 pulses/sec and with a pulse width of 30 ns to minimize pulse overlap effect [4]. The neutron pulses pass through a cylindrical shaped boron filter with dimensions of 8 cm in diameter and 0.04 cm in length (density:  $2.34 \text{ g/cm}^3$ ) and 2.5 cm thick borated polyethylene shielding (density:  $0.95 \text{ g/cm}^3$ ) eliminating the low energy (thermal) tail in the spectrum since the boron has very high probability to absorb thermal neutrons [1,2,5]. As a result, well-defined neutron pulses were injected into a rectangular nuclear graphite pile with dimensions of  $70 \text{ cm (W)} \times 70 \text{ cm (L)} \times 70 \text{ cm (H)}$ . The density of nuclear graphite was determined to be  $1.66583 \pm 0.00004 \text{ g/cm}^3$  [5]. The detector is a lithium glass scintillator with 1 mm thickness and a diameter of 3 inches [1,2]. Figure 1 shows a schematic of the experimental setup.

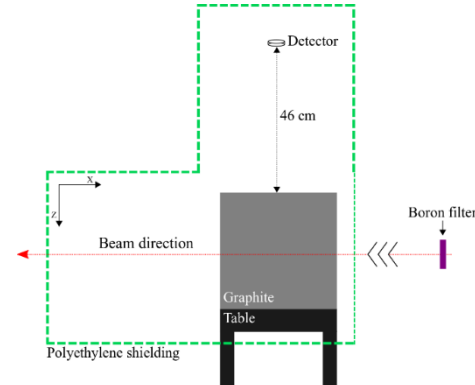


Figure 1. A schematic of the graphite experiment as set up at the ORELA facility.

Finally, the neutrons leaking from the graphite pile were counted by the detector that was placed at a distance of 46 cm from the top surface of the pile. The graphite pile is based on assuming that the neutron time-energy coupling is preserved for the leaking neutrons as it is for the internal

field of the slowing down medium. In this case, the time dependent reaction rate per atom (response of the neutron detector) is given by

$$R(t) = \int_E \sigma(E) \cdot \phi(E, t) dE, \quad (2)$$

where  $\sigma(E)$  is the microscopic cross section for the detection reaction, and  $\phi(E, t)$  is the time-energy dependent neutron flux at the detector.

### Time-Energy Calibration

In order to determine a link between the time and energy of the neutrons during the slowing down process, two sets of detectors were prepared. Data for each set were acquired independently but with the same data acquisition system. The first data set measured the response of a bare detector. The second data set measured the response of the detector covered with a 1 mm thick cadmium sheet. The cadmium cut-off is approximately 0.5 eV, and neutrons with energy below the cadmium cut-off will be absorbed. This calibration was used to verify the computationally (benchmark model) established time-energy correlation and to interpret the measurement.

### Measurement Results

The results of measurement are obtained as energy dependent time distributions of total neutron counts leaking from the graphite pile. Figure 2 shows the measured energy dependent slowing-down-time spectra for the top detector. The measurement period is 1 hour. By identifying the time-energy coupling that is established during neutron slowing down and thermalization in graphite, the response of the detector (i.e., counts) at a given time after the injection of the pulse into the pile can be correlated to the energy of the neutrons at that time. As it can be seen in Fig. 2, two sets of experimental data are presented. The black points indicate the first set corresponding to the response of a bare detector. The red points indicate the second set corresponding to the response of the detector covered with a 1 mm thick cadmium sheet. The measurement results are given with the statistical uncertainties, which were calculated based on Poisson distribution. The use of the cadmium sheet allowed establishing a link between the energy and time of the neutrons during the slowing down process. Specifically, the data shows that the response of the cadmium covered detector is reduced at the time of 75  $\mu$ s after the pulse. It represents an indication that the neutron in the pile have reached an average energy of approximately 0.5 eV, which represents the cut-off energy for the 1 mm thick Cd sheet. As shown by the black points in Fig. 2, this graphite pile gives the higher response after  $1 \times 10^{-4}$  sec, i.e., the time

after which the neutrons have been thermalized to sub-cadmium energies. In the time period  $2.5 \times 10^{-4}$  to  $1.5 \times 10^{-3}$  seconds, a peak region is observed, which correlates to thermal energies as described by Maxwell-Boltzmann statistics. The maximum statistical uncertainty in the black points is on the order of  $\pm 0.7\%$ .

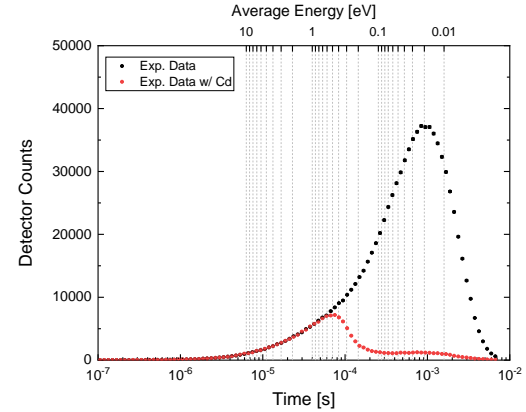


**Figure 2.** The measured slowing-down-time spectra with (red) and without (black) a 1 mm Cd sheet.

### ORELA BENCHMARK SIMULATIONS

Using ORELA benchmark model created to represent the neutron slowing down experiment in graphite, the impact of the suite of graphite thermal scattering cross sections can be selected and compared with measurement results. These calculations were completed using MCNP6.1 code, a Monte Carlo simulation using continuous energy cross sections from both ENDF-B/VII.1 and ENDF/B-VIII.0 [6,7,8]. All MCNP calculations were evaluated using 5000 active cycles, and 10,000,000 particle histories per cycle to achieve a statistical absolute uncertainty of  $\pm 0.3\%$  in the peak region.

The calculations were executed using a combinatorial geometry that is identical to the experimental setup according to the description given in Fig. 1. The model was based on introducing a neutron pulse and monitoring the time-energy dependent neutron flux in a detector. A source emits a neutron pulse at the outside (position:  $x = 1066$  cm,  $y = 0$  cm,  $z = 0$  cm) of a rectangular graphite assembly. The detector is placed outside the assembly at a distance of 46 cm from the top surface of the assembly. The neutron flux in the detector is tallied by using track length estimator (denoted as F4 tally for MCNP6.1 code). The tallied neutron flux is folded with the  $^{6}\text{Li}$  absorption cross section in order to calculate the reaction rate.

### Impact of Carbon Free Gas Treatment

The calculation was completed using the evaluated nuclear data libraries ENDF/B-VII.1 using free gas treatment and the natural carbon cross section library [7].

Using the same ORELA benchmark model, the ENDF/B-VIII.0 was substituted with free gas treatment and natural carbon split with 98.9%  $^{12}\text{C}$  and 1.1%  $^{13}\text{C}$  [8].

### Impact of the Graphite Thermal Scattering Law

A thermal scattering law (TSL) is necessary to accurately capture the graphite cross section. In both ENDF/B-VII.1 and ENDF/B-VIII.0, graphite thermal scattering libraries are available for crystalline (i.e., ideal) graphite. Given the density of the reactor-grade graphite which is significantly lower than the density of the ideal crystalline structure, the porous graphite implemented in ENDF/B-VIII.0 was used to accurately represent the experimental system. The porosity of graphite can be expressed as

$$\text{Porosity (\%)} = \left( 1 - \frac{\rho_{\text{component}}}{\rho_{\text{ideal graphite}}} \right) \times 100, \quad (3)$$

where  $\rho$  is the density of the graphite component or the ideal graphite density. In ENDF/B-VIII.0, nuclear graphite thermal scattering libraries are available for 10% and 30% porous graphite. Additionally, a 20% porous graphite library was tested in this work

The calculations were completed for free gas treatment and using thermal scattering libraries to assess the impact on calculated results, particularly in the peak region. The calculated spectra were normalized based on the high energy range (small times) where it is expected that the same total counts would be recorded by the detector for all measurement conditions. The most appropriate normalization factor is determined by the ratio of C/E being close to 1. The experimental values were compared in Figs. 3-9, separately. In these figures, the experimental data is represented with closed black circles with statistical error bars. The calculated results are plotted as a black histogram. As it can be seen, in Figures 3-4, both calculations using free gas treatment and the carbon cross section libraries overestimate the detector response in the peak region, which corresponds to the low (thermal) energies range from approximately 0.1 to 0.01 eV. As it can be seen, in Figures 5-6, the calculations using the ideal crystalline graphite TSLs underestimate and does not represent the detector response in the peak region. This implies that the nuclear graphite TSLs are essential to capture thermalization effects. In Figures 7-9, the calculation using the nuclear graphite TSLs accurately captures the detector response in the peak region. The 30% porosity graphite TSL shows the most agreement with the experimental data. As the porosity increases from ideal crystalline to 30% porosity, the calculated results demonstrate the impact of the graphite structure on neutron thermalization.

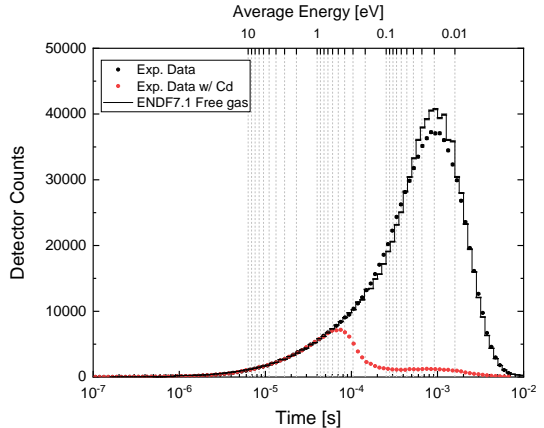


**Fig. 3. Comparison of experimental result of neutron slowing-down-time spectrum and calculation with ENDF/B-VII.1 natural carbon library.**

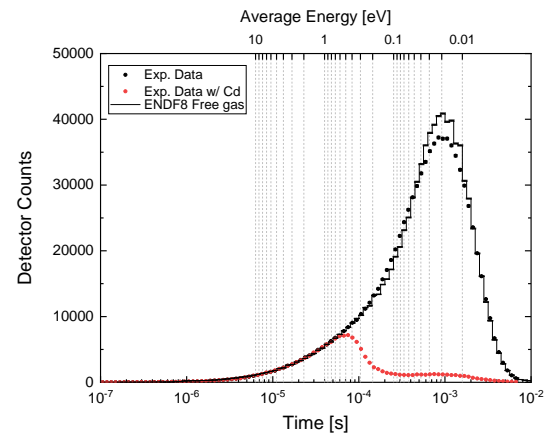


**Fig. 4. Comparison of experimental result of neutron slowing-down-time spectrum and calculation with ENDF/B-VIII.0 natural carbon (split with 98.9%  $^{12}\text{C}$  and 1.1%  $^{13}\text{C}$ ) library.**

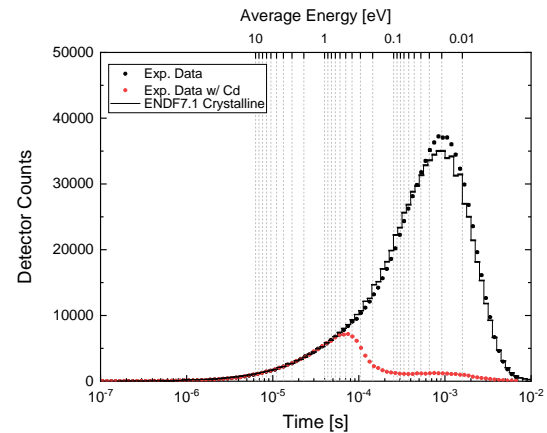


**Fig. 5. Comparison of experimental result of neutron slowing-down-time spectrum and calculation with ENDF/B-VII.1 crystalline graphite TSL.**

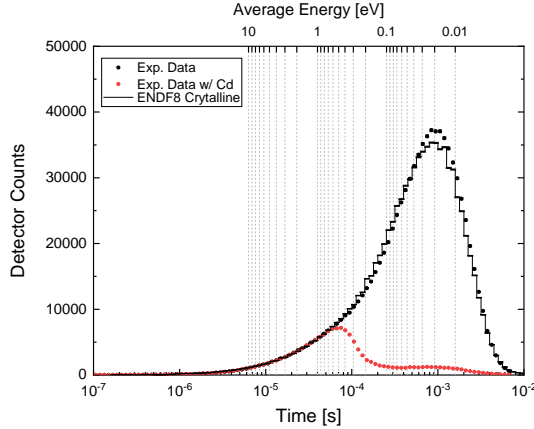


**Fig. 6. Comparison of experimental result of neutron slowing-down-time spectrum and calculation with ENDF/B-VIII.0 crystalline graphite TSL.**

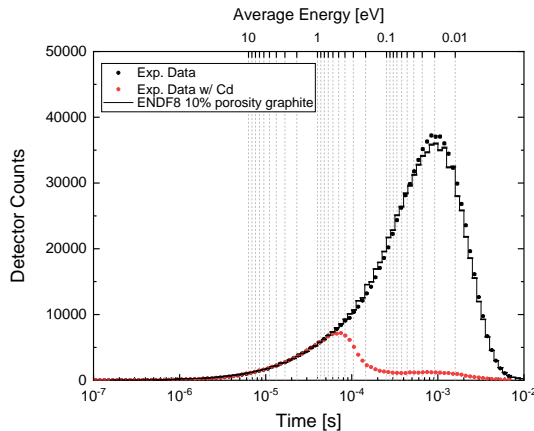


**Fig. 7. Comparison of experimental result of neutron slowing-down-time spectrum and calculation with ENDF/B-VIII.0 10% porosity graphite TSL.**

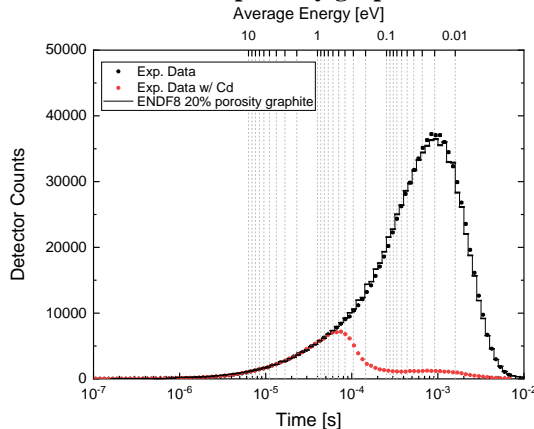


**Fig. 8. Comparison of experimental result of neutron slowing-down-time spectrum and calculation with ENDF/B-VIII.0 20 % porosity graphite TSL.**

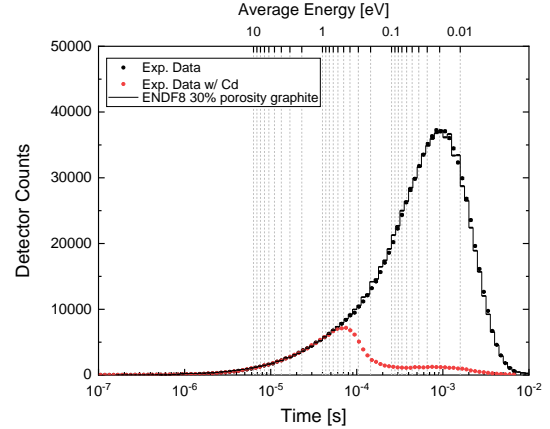


**Fig. 9. Comparison of experimental result of neutron slowing-down-time spectrum and calculation with ENDF/B-VIII.0 30% porosity graphite TSL.**

The deviation between the experimental result and calculated result averaged over the peak region of the time spectra for each of these various cross section libraries is given in Table 1. Using the 30% porosity of nuclear-grade graphite implemented in ENDF/B-VIII.0 shows the best agreement between the ORELA benchmark model and experimental measurement.

**TABLE 1. Deviation of the ORELA benchmark model compared with experimental data at times corresponding to the thermal energy range (0.1 to 0.01 eV) using various cross section libraries.**

Data Library	Mean Absolute Deviation (%)
<hr/>	
Free-gas treatment	
ENDF/B-VII.1 <sup>nat</sup> C	+6.60
ENDF/B-VIII.0 <sup>12</sup> C + <sup>13</sup> C	+6.70
<hr/>	
Graphite TSLs	
ENDF/B-VII.1 <sup>nat</sup> C	-4.35
+ TSL (crystalline graphite)	
ENDF/B-VIII.0 <sup>12</sup> C + <sup>13</sup> C	-3.81
+ TSL (crystalline graphite)	
ENDF/B-VIII.0 <sup>12</sup> C + <sup>13</sup> C	-2.66
+ TSL (10% porosity graphite)	
ENDF/B-VIII.0 <sup>12</sup> C + <sup>13</sup> C	-1.82
+ TSL (20% porosity graphite)	
ENDF/B-VIII.0 <sup>12</sup> C + <sup>13</sup> C	-1.44
+ TSL (30% porosity graphite)	

## CONCLUSIONS

Neutron pulsed Slowing-Down-Time spectrometry is utilized to benchmark the slowing down characteristics and thermalization of neutrons in reactor-grade graphite. Experimental measurement using a  $70 \times 70 \times 70$  cm<sup>3</sup> rectangular nuclear graphite pile was conducted at the ORELA facility of ORNL. The benchmark model was used

to validate for the appropriate graphite library showing good agreement between calculated and experimental data. The calculations were completed using the MCNP code and continuous energy cross sections from both ENDF-B/VII.1 and ENDF/B-VIII.0 for all free gas treatment and thermal scattering libraries. Using the ENDF/B-VIII.0 libraries, the porous nuclear graphite data generally improves agreement with the results of the measurement. Specifically, the 30% porosity nuclear graphite TSL library gives the best agreement with experimental data.

## ACKNOWLEDGMENTS

This work is partially funded by the US DOE through the Nuclear Energy University Program (NEUP).

## REFERENCES

1. A. I. Hawari, B. W. Wehring, "Observation of Neutron Thermalization in Graphite using the Slowing-Down-Time Technique," PHYSOR 2014 – The Role of Reactor Physics Toward a Sustainable Future, Kyoto, Japan (2014).
2. A. I. Hawari, J. L. Wormald, C. A. Manring, "Testing of Graphite Thermal Neutron Scattering Law Data in Support of TREAT Neutronic Analysis," *Transactions of the American Nuclear Society* **115**, 1401 (2016).
3. A. I. Hawari, "Modern Techniques for Inelastic Thermal Neutron Scattering Analysis," *Nuclear data sheets* **118**, 172-175 (2014).
4. K. H. Guber, *et al.*, "Recent Refurbishment of the Oak Ridge Electron Linear Accelerator Neutron Source," United States, (Jan 1, 2008).
5. T. Zhou, "Benchmarking Thermal Neutron Scattering in Graphite," PhD dissertation, North Carolina State University, 2007.
6. T. Goorley, *et al.*, "Initial MCNP6 Release Overview," *Nuclear technology* **180**, 298-315 (2012).
7. M. B. Chadwick, *et al.*, "ENDF/B-VII.1 Nuclear Data for Science and Technology: Cross Sections, Covariances, Fission Product Yields and Decay Data," *Nuclear data sheets* **112**, 2887 (2011).
8. D. A. Brown, *et al.*, "ENDF/B-VIII.0: The 8th Major Release of the Nuclear Reaction Data Library with CIELO-Project Cross Sections, New Standards and Thermal Scattering Data," *Nuclear data sheets* **148**, 1-142 (2018).